COMPENSATING THE EFFECT OF ASYMMETRICALLY PLACED UNDULATORS IN FODO LATTICES

J. Zemella*, P. Niknejadi, M. Vogt, Deutsches Elektronen-Synchrotron DESY, Hamburg, Germany
Z. Chen, B. Faatz, Shanghai Advanced Research Institute, Pudong, China

Abstract

The dynamical focusing of FEL undulators with variable gap in FODO lattices with varying but overall low energy is detrimental to the FODO optics. In the absence of compensation by adjusting the FODO quadrupole strengths it may drive the cell unstable. Typical examples of FELs in the critical regime are FLASH at DESY and the SXFEL-SBP at the Shanghai Synchrotron Radiation Facility. Before, in our contributions to FEL 2024 and IPAC 2025 we have extensively discussed the case where the undulators are centered inside the FODO drift of a Lattice with symmetric FODO cells. Here we treat the fairly common case where the drifts on each side of the undulator are unequal, which has significant impact on the compensation strategy and stability issues.

INTRODUCTION

In Ref. [1] we have discussed the effect of the transverse focusing of undulator insertions on the electron optics of FODO structures designed to stabilize the beam transport through the long undulator sections of Free Electron Lasers (FELs). At low beam energy in particular, the pre-matched optics (e.g. for open gaps / vanishing undulator strength) may become unstable. The Shanghai Soft X-Ray Free Electron Laser Facility (SXFEL) [2, 3] at the Shanghai Synchrotron Radiation Facility (SSRF), and the Free electron LASer in Hamburg (FLASH) [4–6] at DESY – also in its upgraded form [7–9] – can operate in this potentially unstable regime. The topic has been treated before by various groups [10–12], but not at this generality. Following Refs. [1, 13], we refer to FODO cells with undulators inserted into the "O"-drifts as "FUDU" cells. In Ref. [1] we presented stability criteria and a numerical scheme to maintain an initially matched optics under variation of the undulator strengths. In Ref. [13] we derived a quasi-analytical match-preservation scheme for exactly mirror-symmetric "fUDUf" cells[1], i.e. cells with two identical undulators and identical up- and downstream drifts surrounding each undulator. There, the match-preservation conditions reduce to the real zeros of a polynomial of order of 4 in θ_f.

In most FUDU designs, however, the up- and downstream drifts surrounding each undulator are not identical, breaking the mirror symmetry of the individual insertion. In the present contribution we generalize the scheme of Ref. [13] to this practically relevant asymmetric case. Figure 1 gives a sketch of our our asymmetric fUDUf scheme, and illustrates

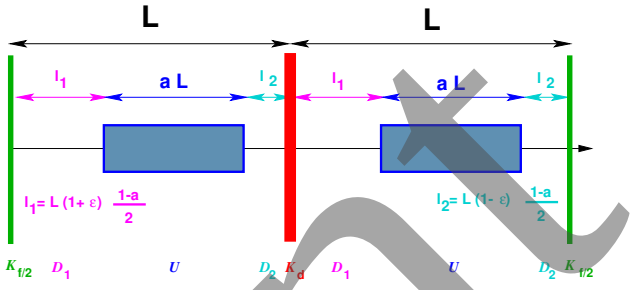

Figure 1: Schematic drawing of an asymmetric fUDUf cell, illustrating our notation.

the meaning of the half-cell length L, as well the filling factor a and the asymmetry parameter ϵ. The match-preservation conditions now yield a polynomial of order of 8 in θ_f, whose roots can be computed easily numerically.

STABILITY ASPECTS OF THE PLANAR ($\theta_{Ux} \equiv 0$) FUDUF

In their 2012 paper [11] Quattromini et al. proposed that undulator focusing should drive the optics of the underlying focusing structure unstable for undulator strengths in certain bands. Here we adopt the cell normal form coordinates and the dimensionless scaled kick strengths $\theta_n := \kappa_n L := k_n l_n L$ ($n = f, d, Ux, Uy$) of Refs. [1, 13], with the k_n, l_n being the "conventional" focusing strengths, and the element lengths respectively, and use throughout the dimensionless β-functions $\bar{\beta}_i := \beta_i / L$ ($i = x, y$), with L the half length of the FODO cell. Moreover, we re-use the notations for matrices representing the thin lens quadrupoles $\underline{K}_f$, $\underline{K}_d$, the drifts $\underline{D}_{l/L}$ of length l, and the (thick lens, planar horizontally wiggeling) undulator $\underline{U}_{a,\theta_{Ux},\theta_{Uy}}$ of length aL, and independent scaled focusing kicks θ_{Ux} and θ_{Uy} (here: $\theta_{Ux} \equiv 0$).

Two of us [12] have analyzed the assertion of Ref. [11] by introducing a parametrization of the half-cell maps using two functions $A_{a,\epsilon}(\theta_{Uy})$, and $B_{a,\epsilon}(\theta_{Uy})$.[2] This parametrization, which factors out the scaled quadrupole kick strengths θ_f and θ_d, enables certain conclusions on the stability of the full fUDUf map $\underline{C}^*$. In particular, it turns out that trace $\underline{C}^*$ is independent of θ_f and θ_d, whenever $A_{a,\epsilon}(\theta_{Uy}) = 0$. Moreover $|\text{trace}\, \underline{C}^*| \leq 2$ then requires that $|B_{a,\epsilon}(\theta_i)| \leq 1$ for the zeros θ_i of $A_{a,\epsilon}$. As usual, the case $|\text{trace}\, \underline{C}^*| = 2$ (here $|B_{a,\epsilon}(\theta_i)| = 1$) must be treated with some extra care. See e.g. Ref. [1]. When $a = 1$, $\underline{C}^*$ is independent of ϵ and we choose $\epsilon = 0$. Then $A_{1,0}$ has zeros at $\theta_n = n^2\pi^2$, $n \in \mathbb{N}_*$. These θ_n are at the same time maxima of $B_{1,0}$ with $B_{1,0}(\theta_n) = 1$. Numerical studies indicate that $\underline{C}^*(a = 1, \theta_{Uy}; \theta_f, \theta_d)$ has a

* johann.zemella@desy.de

[1] We restrict ourselves to fUDUf cells for brevity, but it is clear that analogue results can be derived for dUFUd cells.

[2] In the original paper A and B are functions of $\xi := \sqrt{\theta}$.

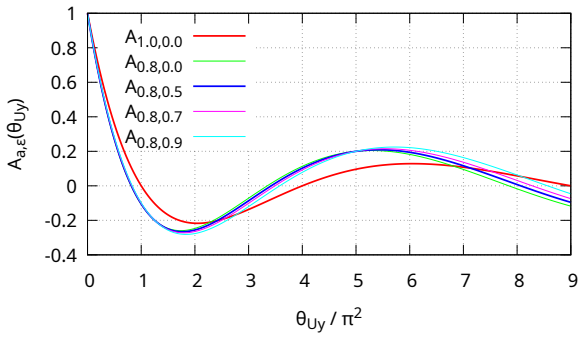

Figure 2: The $A_{a,\epsilon}$-function [12] for some useful values of a, and ϵ. The red curve represents the case of vanishing drifts where the zeros can calculated easily analytically to $n^2\pi^2$. Here: $n_0 = 1, 2, 3$. The blue curve is for a filling factor of $a = 0.8$ and an asymmetry $\epsilon = 0.5$ which is discussed below.

domain of stability $\mathscr{S}_{1,0}(\theta_{Uy})$ with non-vanishing measure in θ_f/θ_d-space whenever $\theta_{Uy} \neq \theta_n$. The shape of $\mathscr{S}_{1,0}$ varies smoothly with θ_{Uy} unless it crosses θ_n where the shape changes discontinuously. Close to $\theta_{Uy} = \theta_n$ cell map has a finite $\mathscr{S}_{1,0}$ but the phase advances and Twiss functions become "unfriendly" (μ close to 2π, β's at quads extremely small, etc.), so one wants to avoid these "bands of inconvenience". Figure 2 plots the $A_{a,\epsilon}$ function for some customary values of a and ϵ in the range of θ_{Uy} from 0 to $9\pi^2$ in units of π^2. In passing we note that the largest θ_{Uy} found currently relevant in Ref. [1] was $\theta_{Uy} = 3.337$ for the SBP beamline of the Shanghai Soft X-Ray Free Electron Laser Facility [2,3] and is quite a bit smaller than the *characteristic* 1st zero $\pi^2 \approx 9.8696$ of $A_{1,0}(\theta_{Uy})$. For finite $0 < a < 1$, $-1 < \epsilon < +1$ the situation is more complicated. The zeros θ_n of $A_{a,\epsilon}$ are no longer exactly at $n^2\pi^2$. Numerical study show that the system now has real bands of instability where $\mathscr{S}_{a,\epsilon}(\theta_{Uy})$ has zero measure. We note here that $\mathscr{S}$ is the domain of stability of the *complete* 4×4 matrix, i.e. the intersection of $\mathscr{S}^{(x)}$ and $\mathscr{S}^{(y)}$, the domains of stability in θ_f/θ_d-space of the the horizontal (FODO) and vertical (FUDU) 2×2 matrices respectively. Thus $\mathscr{S} = \emptyset$ can mean $\mathscr{S}^{(y)} = \emptyset$ as well as $\mathscr{S}^{(y)} \neq \emptyset$ but $\mathscr{S}^{(y)} \cap \mathscr{S}^{(x)} = \emptyset$.[3] Figure 3 illustrates the changes of $\mathscr{S}_{0.8,0.5}$ when θ_{Uy} approaches the unstable band $\sim (8.06, 8.09)$.

Any quadrupole scheme (in θ_f/θ_d-space) to compensate the variable undulator focusing strength must somehow stay inside $\mathscr{S}_{a,\epsilon}(\theta_{Uy})$ over the complete θ_{Uy}-range it is supposed to cover.

COMPENSATION SCHEME FOR THE ASYMMETRIC FUDU

We generalize the cell $\underline{A}$ of Eq. (3) of Ref. [13] to cells with non-identical up- and downstream drifts surrounding

[3] $\mathscr{S}^{(x)} \equiv \mathscr{S}^{(2\times2,\text{fodo})}$ is independent of θ_{Uy} and never empty.

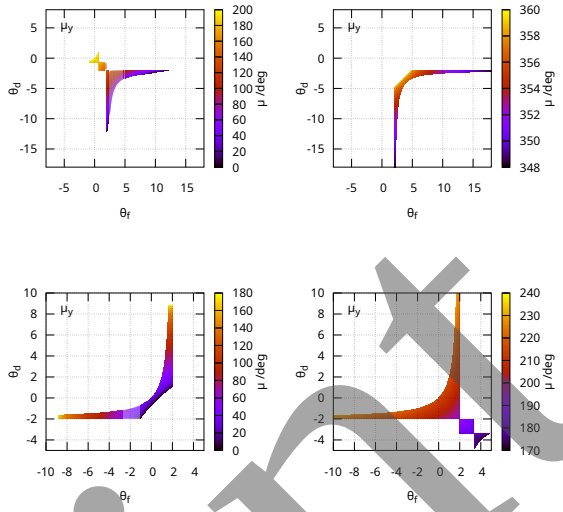

Figure 3: The Domains $\mathscr{S}_{a,\epsilon}(\theta_{Uy})$ of stability in θ_f/θ_d-space of $\underline{C}^*$ in the case of $a = 0.8$ and $\epsilon = 0.5$. $\mathscr{S}_{a,\epsilon}(\theta_{Uy})$ is colored in a color scheme decoding the vertical phase advance μ_y per cell. It's complement is colored in white. Top left: $\theta_{Uy} = 3.00$; top right: $\theta_{Uy} = 8.04$; bottom left: $\theta_{Uy} = 13.0$; bottom right: $\theta_{Uy} = 25.0$. $\mathscr{S}_{0.8,0.5}(\theta_{Uy})$ is nonempty for $\theta_{Uy} < 8.06$ or $8.09 \leq \theta_{Uy}$. We found that inside this band $\mathscr{S}^{(x)}_{0.8,0.5}$ and $\mathscr{S}^{(y)}_{0.8,0.5}$ do not overlap and that the $\mathscr{S}^{(y)}_{0.8,0.5}(\theta_{Uy})$ approaches infinitely large $\theta_{f/d}$s when θ_{Uy} approaches its 1st zero of $A_{0.8,0.5}$ (≈ 8.063). The examples have been chosen to illustrate the smooth variation of the domain shapes away from the 1st zero of $A_{0.8,0.5}$.

each undulator ($\underline{A} \to \underline{B}$),

$$\underline{B} := \underline{D}_{\Lambda(1+\epsilon)}\, \underline{U}_{a,\theta_{Ux},\theta_{Uy}}\, \underline{D}_{\Lambda(1-\epsilon)}\,, \quad -1 \leq \epsilon \leq +1\,, \quad (1)$$

with $\Lambda = (1-a)/2$, while keeping $\underline{B}_{\text{upstr.}} \equiv \underline{B}_{\text{downstr.}}$. The fUDUf cell map then reads

$$\underline{C}^* = \underline{K}_{+\theta_f/2}\, \underline{B}\, \underline{K}_{-\theta_d}\, \underline{B}\, \underline{K}_{+\theta_f/2}\,. \quad (2)$$

For $\epsilon \neq 0$ the individual insertion $\underline{B}$ is no longer mirror-symmetric in the sense of Ref. [13], $\underline{S}\,\underline{B}^{\mathrm{T}}\,\underline{S} \neq \underline{B}$, and the lemma proved in the appendix of Ref. [13] does not apply. Consequently $\alpha_x, \alpha_y \not\equiv 0$ at the cell boundaries, and an initial match with $\alpha^i_{x,y} = 0$ (for $\theta_{Uy} \equiv 0$, i.e. $\underline{B} \equiv \underline{A} \equiv \underline{D}_L$) cannot be strictly preserved under variation of the undulator strengths.

Instead we relax the matching requirement: we demand only that the $\bar{\beta}$-functions at the cell boundary be preserved,

$$\bar{\beta}^{out}_{x,y} \stackrel{!}{=} \bar{\beta}^{in}_{x,y} =: \bar{\beta}_{x,y}, \quad (3)$$

while allowing $\alpha^{out}_{x,y} \neq 0$. The residual mismatch [14] is then quantified for each plane, by

$$\lambda_i = \tfrac{1}{2}\left(\frac{\bar{\beta}^{out}_i}{\bar{\beta}^{in}_i} + \frac{\bar{\beta}^{in}_i}{\bar{\gamma}^{out}_i}\right), \quad i = x, y, \quad (4)$$

with $\alpha_i^{in} = 0$, which we use as initial match into the mirror symmetric FODO cell with $\theta_{Uy} = 0$.

The condition $\bar{\beta}_i^{out} = \bar{\beta}_i^{in}$ together with periodicity of the trace yields, for each plane , the polynomial constraint

$$\left(\frac{\operatorname{trace} \underline{C}^{(i)\star}}{2}\right)^2 + \left(\frac{\underline{C}_{12}^{(i)\star}}{\bar{\beta}_i}\right)^2 = 1, \quad i = x, y, \tag{5}$$

obtained by eliminating μ_i via $\cos^2 \mu_i + \sin^2 \mu_i = 1$ from $\operatorname{trace} \underline{C}^{(i)\star} = 2\cos\mu_i$ and $\underline{C}_{12}^{(i)\star} = \bar{\beta}_i \sin\mu_i$. This form is purely polynomial in (θ_f, θ_d) and free of the sign ambiguities of $\cos\mu_i$ and $\sin\mu_i$ which would otherwise generate spurious branches.

A direct degree count gives: $\operatorname{trace} \underline{C}^{(i)\star}$ and $\underline{C}_{12}^{(i)\star}$ are each linear in θ_d and quadratic in θ_f.[4] Eq. (5) is therefore quadratic in θ_d and quartic in θ_f for both planes. Solving the x-equation for $\theta_d(\theta_f)$ (two branches from the quadratic in θ_d) and substituting into the y-equation yields a rational equation

$$0 = \frac{P_{\underline{B}}^{(8)}(\theta_f)}{P_{\underline{B}}^{(k)}(\theta_f)}, \tag{6}$$

whose numerator $P_{\underline{B}}^{(8)}$ is a polynomial of order 8 in θ_f. Real roots of $P_{\underline{B}}^{(8)}$ at which the denominator does not vanish provide up to 8 candidate values for θ_f; the corresponding θ_d follows by back-substitution. The roots can be easily calculated numerically.

The numerator $P_{\underline{B}}^{(8)}$ generically yields up to 8 roots in $\mathbb{C}$, of which typically only one or two are physically relevant. The reduction to $P_{\underline{B}}^{(8)}$ involves squaring twice in order to eliminate the $\sqrt{\cdot}$ terms arising from $\cos\mu_i = \pm\sqrt{1-\sin^2\mu_i}$, which introduces spurious roots corresponding to wrong sign combinations of $\sin\mu_i$ and $\cos\mu_i$. The physically relevant root is identified by:

1. $|\Im(\theta_f)| = 0$
2. non-vanishing denominator, $P_{\underline{B}}^{(k)}(\theta_f) \neq 0$;
3. periodicity of the residual α, i.e. $\alpha_i^{out} = \alpha_i^{in}$ for $i = x, y$;

As in the symmetric case [13], proximity of a candidate root to a zero of $P_{\underline{B}}^{(k)}$ signals enhanced sensitivity to the input parameters and may require switching between branches of the parametrizations of $\theta_f(\theta_{Uy})$ and $\theta_d(\theta_{Uy})$. Most likely this happens when either $\theta_f(\theta_{Uy})$ or $\theta_d(\theta_{Uy})$ get close to the boundary of $\mathscr{S}(\theta_{Uy})$.

RESULTS FOR ASYMMETRIC FUDUS

We illustrate the asymmetric compensation scheme with two identical planar undulators ($\theta_{Ux} = 0$, $\theta_{Uy} \neq 0$) and fill factor $a = 0.8$. The initial match corresponds to unperturbed phase advances $\mu_x = \mu_y = 60°$, with the open-gap solution as reference. We compare the symmetric configuration ($\epsilon = 0$, identical up- and downstream drifts) with asymmetric ones ($\epsilon = 0.4, 1$).

Figure 4 (top) shows that the physically selected root of $P_{\underline{B}}^{(8)}(\theta_f)$ varies smoothly with the undulator strength over the full scanned range $\theta_{Uy} \in [0, 4]$. Both θ_f and θ_d shift noticeably between the symmetric and the asymmetric configurations, demonstrating that the static (open-gap) quadrupole strengths are no longer sufficient when $\epsilon \neq 0$. The corresponding traces in Fig. 4 (bottom) remain within the stability band $|\mathrm{Tr}/2| < 1$ over the entire range, confirming that the compensated cell is stable in both planes. But for larger undulator focusing the values are close to 1 in certain regions for certain branches.

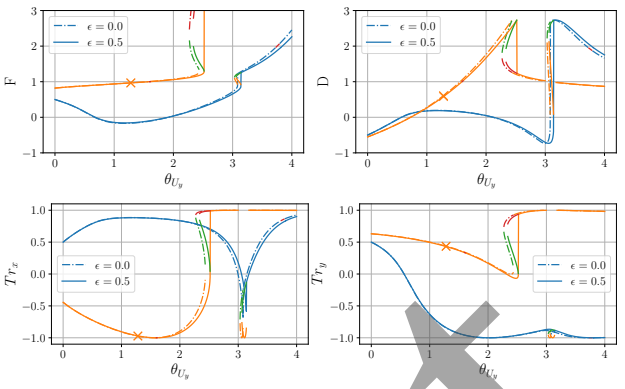

Figure 4: Compensation solution and resulting cell stability for $a = 0.8$, $\mu_x = \mu_y = 60°$, planar undulator. Top: physically selected root θ_f, θ_d of $P_{\underline{B}}^{(8)}$ as a function of θ_{Uy}. Bottom: half-trace trace $\underline{C}^{(i)\star}/2$ in both planes; stability requires $|\mathrm{trace}/2| < 1$. Shown for the symmetric ($\epsilon = 0$) and asymmetric ($\epsilon = 0.4$) drift configurations.

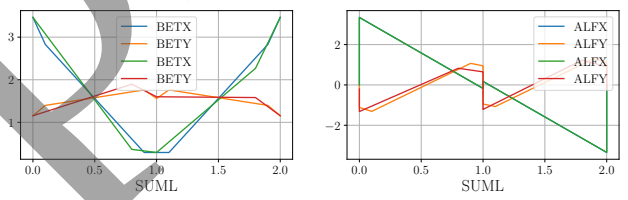

Figure 5: $\bar{\beta}_{x,y}(s)$ (top) and $\alpha_{x,y}(s)$ (bottom) across one compensated cell at $\theta_{Uy} = 1.5$, $\epsilon = 0.4$. The asymmetric drift configuration breaks the cell mirror symmetry, producing nonzero $\alpha_{x,y}$ at the cell boundaries while $\bar{\beta}_{x,y}^f = \bar{\beta}_{x,y}^{in}$ is preserved by construction.

Figure 5 illustrates the consequence of the broken mirror symmetry on the Twiss functions: while $\bar{\beta}_{x,y}$ returns to the initial value at the end of the cell — this is the very condition imposed by Eq. (5) — the $\alpha_{x,y}$-functions are nonzero at the boundaries, in contrast to the symmetric case where $\alpha_{x,y}^{in} = 0$ holds exactly. The residual mismatch λ_y between the realized periodic optics and the open-gap reference grows monotonically with θ_{Uy}, from unity at vanishing undulator strength up to $\lambda_y \approx 1.5$ at $\theta_{Uy} = 4$ for $\epsilon = 1.0$, and remains within tolerable bounds across the full operational range.

REFERENCES

[1] J. Zemella, M. Vogt, B. Faatz, and Z. Chen, "Automatic Electron Optics Compensation for FODO Lattices Affected by Undulator Focusing", presented at FEL'24, Warsaw, Poland, Aug. 2024, paper TUP124.

[4] dUFUd: linear in θ_f and quadratic in θ_d.

[2] Z. T. Zhao *et al.*, "Status of the SXFEL facility", *Appl. Sci.*, vol. 7, no. 6, p. 607, 2017. doi:10.3390/app7060607

[3] J. D. Fan *et al.*, "First commissioning results of the coherent scattering and imaging endstation at the Shanghai soft X-ray free-electron laser facility", *Nucl. Sci. Tech.*, vol. 33, no. 114, 2022. doi:10.1007/s41365-022-01103-0

[4] W. Ackermann *et al.*, "Operation of a free-electron laser from the extreme ultraviolet to the water window", *Nat. Photonics*, vol. 1, pp. 336–342, 2007. doi:10.1038/nphoton.2007.76

[5] M. Vogt *et al.*, "FLASH Status 2024 — FEL Operation for Users and Upgrade Shutdown", in *Proc. IPAC'25*, Taipei, Taiwan, Jun. 2025, pp. 102–105. doi:10.18429/JACoW-IPAC2025-MOPB019

[6] K. Honkavaara and S. Schreiber, "FLASH: The Pioneering XUV and Soft X-Ray FEL User Facility", in *Proc. FEL'19*, Hamburg, Germany, Aug. 2019, pp. 734–737. doi:10.18429/JACoW-FEL2019-THP074

[7] M. Beye *et al.*, "FLASH2020+, Conceptual Design Report", DESY, Hamburg, Germany, Rep. PUBDB-2020-00465, Mar. 2020. doi:10.3204/PUBDB-2020-00465

[8] L. Schaper *et al.*, "Transformation of FLASH1 to a High Repetition Rate Externally Seeded FEL for Users", presented at FEL'24, Warsaw, Poland, Aug. 2024, paper TUAC02.

[9] E. Ferrari *et al.*, "Better a Chicane Today than an Undulator Tomorrow", presented at FEL'24, Warsaw, Poland, Aug. 2024, paper TUBI01.

[10] B. Faatz *et al.*, "The FLASH Facility: Advanced Options for FLASH2 and Future Perspectives", *Appl. Sci.*, vol. 7, p. 1114, 2017. doi:10.3390/app7111114

[11] M. Quattromini *et al.*, "Focusing Properties of Linear Undulators", *Phys. Rev. ST Accel. Beams*, vol. 15, p. 080704, 2012. doi:10.1103/PhysRevSTAB.15.080704

[12] Z. Chen and B. Faatz, "Automatic Adjustment of Undulator Optics for FELs", *arXiv*, 2024. doi:10.48550/arXiv.2405.08339

[13] J. Zemella, L. Schaper, M. Vogt, B. Faatz, Z. Chen, and P. Amstutz, "Parametric Optics for FUDU Lattices with Strongly Focusing Undulators", in *Proc. IPAC'25*, Taipei, Taiwan, Jun. 2025, pp. 2211–2214. doi:10.18429/JACoW-IPAC2025-WEPM100

[14] M. G. Minty and F. Zimmermann, *Measurement and Controll of Charged Particle Beams*, Heidelberg, Germany: Springer-Verlag Berlin, 2003. doi:10.1007/978-3-662-08581-3